Phase Studies by Diffusive Interfacial Transport Using Near-Infrared Analysis for Water (DIT-NIR)

Robert G. Laughlin, Matthew L. Lynch,* C. Marcott, Richard L. Munyon, Albert M. Marrer, and Kelly A. Kochvar

Miami Valley Laboratories, The Procter & Gamble Company, Cincinnati, Ohio 45253-8707

Received: November 30, 1999; In Final Form: May 8, 2000

The Diffusive Interfacial Transport (DIT) method for performing phase studies (in which all the phases that exist along an isotherm are produced by isothermal swelling and their compositions determined by using refractive index data) was introduced in 1987.[1] While this method represented a significant qualitative advance in phase studies methodology, its quantitative accuracy has since been found to be unsatisfactory. We describe herein the DIT-NIR method in which execution of the study is the same as before, but peak-area data on the bend−stretch combination band of water are used to determine composition. Peak-area data are obtained by using Fourier transform near-infrared (FT-NIR) microspectroscopy. Calibration studies with octyldimethylphosphine oxide−water mixtures demonstrated that peak areas vary linearly with composition over the entire composition range. The slopes of calibration lines follow a power-law dependence upon temperature. Phase studies of the $C_{12}E_3$−water system, using both DIT-NIR and isoplethal methods, validate the applicability of the DIT-NIR method to systems other than phosphine oxides. These data suggest that DIT-NIR may represent a new general method for the complete and accurate quantitative determination of binary aqueous surfactant phase diagrams. Further, the spectroscopic data can provide new information on the physical state of the material under study.

Background

The Diffusive Interfacial Transport (DIT) method for the quantitative determination of binary aqueous surfactant phase diagrams was reported in 1987.[1] This is an isothermal swelling method in which water and surfactant are brought into molecular contact within a long, thin, capillary having a rectangular cross section. A long-lived concentration gradient develops along the length of the capillary as a result of diffusive transport. If gaps in miscibility exist, this gradient is interrupted by interfaces. The interfaces reflect the discontinuities in composition that exist across miscibility gaps and divide the contents of the capillary into phase bands. Although composition profiles within each band (which are dictated by swelling dynamics) change with time, the compositions to either side of each interface (which are dictated by thermodynamics) do not. The in situ measurement of compositions at interfaces provides data on the limits of composition of all the phases that exist at the temperature of the study, and studies over a range of temperatures provide the data necessary to construct the entire phase diagram. Data on composition profiles can also yield diffusion coefficients within phase bands and their dependence on composition.[2]

The concentration gradient that spontaneously develops during DIT studies along the length of the cell (termed the *x*-direction) persists for very long times, while gradients in the *y*- and *z*-directions vanish within minutes.[1] This one-dimensional gradient is ideal for the observation and analysis of phase behavior. Being isothermal, the DIT approach sidesteps basic problems that are inherent to all isoplethal methods.[3,4] It is applicable to the study of liquid-crystal-forming surfactants and amphiphilic polymer systems, irrespective of the viscosities of the phases that exist. The contact of metastable phases with water accelerates their collapse to the equilibrium phase;[5] this facilitates the determination of equilibrium phase diagrams.

Swelling methods are compromised only for the specific combination of circumstances that the surfactant is poorly soluble in water and the coexisting phase is a water-rich lamellar liquid crystal. When this specific situation exists (and *only* when it exists), "anomalous swelling" creates a myelin texture within the region of the interface that prevents one from determining the compositions of the coexisting phases.[6,7] Anomalous swelling is closely related to the "spontaneous" formation of colloidal vesicular structure in dilute biphasic mixtures of such compounds.[6]

The main practical limitation of this method is the requirement that the compound being studied be sufficiently stable in its melt to be loaded into the cell without chemical decomposition. This requirement has so far frustrated studies of sodium dodecyl sulfate.

The considerable value of the DIT principle has been firmly established by numerous phase studies, among which those of dioctadecyldimethylammonium chloride (DODMAC),[7−9] dioctadecylammonium cumenesulfonate (DOACS), *N*-dodecanoyl-*N*-methylglucamine (DMG),[5] and lower ethoxylogs of alkyl polyoxyethylene surfactants[1,10] are especially important. In the DODMAC study, the composition of the concentrated boundary of the lamellar liquid crystal phase region was established. In this boundary, cusps at temperatures which correlated with independently determined peritectic phase reaction temperatures of the coexisting crystal hydrates were observed. The composition of the dilute boundary of this region could not be determined because of anomalous swelling discovered during this study.

* Corresponding author. E-mail: lynch.ml@pg.com.

10.1021/jp994220e CCC: $19.00
Published on Web 07/19/2000

The DMG study[4] established that this system displays classical phase behavior, but the temperature observed for the Krafft eutectic was found to be about 50 °C higher than had been suggested by isoplethal data. Further, swelling of the metastable solid formed by rapid cooling of the melt allowed determination of the metastable extension of the hexagonal phase to below the Krafft eutectic temperature. The collapse of metastable solid phases to the equilibrium crystal phase could be observed and the path to equilibrium determined.

The DOACS study (to be published) established unexpectedly that the composition range of the lamellar liquid crystal region in this system is sharply reduced, in comparison with that in the DODMAC−water system. In DODMAC, this phase spans the composition range from 31% to about 95% surfactant (depending on temperature), while in DOACS it is confined to the composition range from about 93% to 100%. Unlike DODMAC, DOACS was found to exist as a *thermotropic* lamellar liquid crystal phase, i.e., a phase of 100% composition. Because DOACS is hydrophilic, its thermotropic phase extends into the binary aqueous diagram (unlike most thermotropic liquid crystal-forming compounds).[11] The same is true of DMG. The vast difference in the composition range of the liquid crystal in these two systems is attributed to the hydrotropic nature of the cumenesulfonate anion.

Studies of poorly water-soluble nonionic surfactants such as $C_{12}E_3$ (trioxyethylene glycol monododecyl ether) disclosed their complex equilibrium phase behavior. In addition, they supplied support for the correlation (noted above) that anomalous swelling and spontaneous vesicles appear only when a dilute lamellar liquid crystal coexists with an aqueous phase that is nearly pure water. The complex aqueous phase behavior of $C_{12}E_2$ was recently determined by using DIT-NIR.[12] DIT studies also demonstrated unambiguously that $C_{12}E_1$ (like $C_{12}E_0$) does **not** display surfactant phase behavior.[10]

In all the above studies, swelling processes could be observed (by using both polarized light and Jamin−Lebedeff illumination) in an optically uniform cell at a well-controlled temperature during time periods ranging from hours to days. Quantitative data on the spans of miscibility gaps (and their dependence on temperature) could be obtained—information that has never previously been available. These studies not only provided reliable equilibrium phase data but, unexpectedly, often revealed new information on nonequilibrium and colloidal phenomena. Indeed, much of the information described above cannot be obtained by using any other phase studies method.

In the original DIT method, composition was estimated from refractive index data obtained by quantitative transmission interferometry, but accurate compositions could not easily be extracted from these data and adjustments had to be made. Interferometry was performed by using a polarized light microscope fitted with Jamin−Lebedeff optics, and very accurate retardation data were obtained by using a significantly improved analysis of Senarmont data.[1,13] Problems had been anticipated in the analysis of birefringent phases since the polarization state of light is altered on passing through these phases to a degree that depends on its phase structure and orientation, as well as on the system variables (composition, temperature, and pressure). These factors were expected to significantly influence the observed refractive index unless easily reproducible orientation was achieved. Unfortunately, good orientation was *not* typically achieved, and these problems proved to be severe.

More surprisingly, the quantitative analysis using index data of isotropic liquid surfactant phases has also been unsatisfactory.

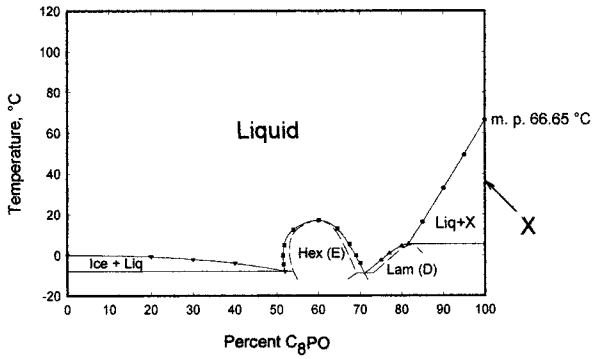

Figure 1. Phase diagram of the octyldimethylphosphine oxide−water system determined by using the isoplethal stepwise dilution (SWD) method.

The refractive indices of sucrose solutions display only gentle curvature vs concentration over a wide composition range, and index data have long been used to determine sucrose concentrations.[14] It was expected that isotropic surfactant solutions would behave similarly, but data on the concentrated liquid in the $C_{12}E_3$−H_2O system suggest otherwise. Excessive curvature in the index-concentration function necessitates extensive calibration and compromises the method. The reason for the excessive curvature of these data is unknown.

The present work was initiated in response to these problems. In developing this new method, the desirable isothermal swelling aspects and optical techniques of the earlier DIT technique were retained, but the quantitation process was greatly improved by using NIR microscopy. This new method will be termed "DIT-NIR", while the older method will henceforth be termed "DIT-NDX".

Experimental Section

In the Supporting Information, the cells, temperature measurement and control, details of the spectral determination of water composition, calibration of spectral data with respect to composition using octyldimethylphosphine oxide (C_8PO), and execution of DIT studies are described. Physical studies of C_8PO and of $C_{12}E_3$ are described below.

Materials Purification and Storage. C_8PO was synthesized by the published method and purified by distillation and recrystallization.[15] The phase diagram of the C_8PO-water system (Figure 1) was determined by using the isoplethal stepwise dilution method.[16] Because C_8PO is extremely stable thermally and is chemically inert, it requires no special storage conditions.

The surfactant $C_{12}E_3$ (the phase behavior of which has been previously reported[10]) was used to evaluate the DIT-NIR principle. Although $C_{12}E_3$ is stable thermally and inert to hydrolysis, it undergoes facile autoxidation (especially when pure), and special purification and storage procedures were therefore developed and used. The best commercially available $C_{12}E_3$ (Fluka) was found by gas chromatographic analysis, with flame ionization detection (GC-FID) after silylating with BTSFA in methylene chloride,[17] to typically assay at about 98%. Figure 2 shows the GC chromatogram of a typical commercially supplied sample, which contains numerous autoxidation products. Impurities at this level are unacceptable for definitive physical studies because they measurably affect phase behavior.[10]

Autoxidation products can be removed by recrystallization from pentane. To recrystallize $C_{12}E_3$ (mp 16.7 °C), a 15% solution in pentane is cooled to −10 °C in a closed, jacketed, mechanically stirred pressure filter to precipitate the surfactant

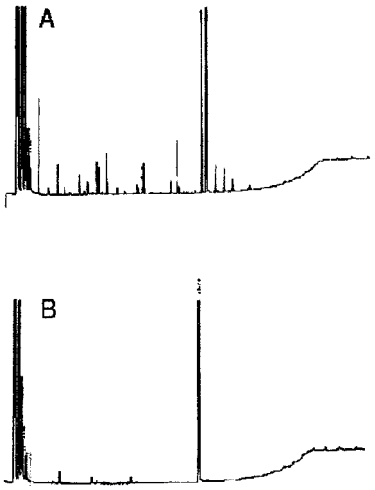

Figure 2. GC−FID analysis of $C_{12}E_3$ before (top) and after (bottom) recrystallization from pentane. The presence of numerous oxidation products in the starting material, and their removal by recrystallization, are clearly shown. The small impurity peaks remaining after recrystallization represent homologue or ethoxylog impurities.

crystals. Sufficient nitrogen pressure is maintained below the frit during this process to keep the slurry above the frit; when filtration is desired, pressure is applied *above* the liquid. The collected crystals are washed with cold pentane (to remove the mother liquor), and the product is recovered by dissolution in pentane at room temperature. The pentane is removed by drying to constant weight *in a vacuum* at room temperature in a rotary evaporator. After two recrystallizations, GC-FID assay of the $C_{12}E_3$ (if free of homologues and ethoxylogs) was typically >99.9%. The purity of the $C_{12}E_3$ was reconfirmed before each phase study.

Once purified, $C_{12}E_3$ must be protected properly because its high purity strongly enhances its reactivity to autoxidation. To do this, the purified sample was promptly subdivided into ca. 100 mg aliquots in 2-cm^3 glass ampules and the ampules attached to a six-arm glass manifold by using rubber tubing. They were degassed *in a vacuum* by using several freeze−thaw cycles between room temperature and a dry ice/acetone bath and then sealed. Large amounts of gas are released in the first cycle, while negligible amounts are released after several cycles. Invisible pinholes may exist in seals. These allow samples to oxidize to a measurable and significant degree, but properly deoxygenated and sealed $C_{12}E_3$ is (as expected) stable at room temperature indefinitely (for years). The unused portions of opened ampules are best stored in a vacuum desiccator at < 0.1 Torr; samples stored in this manner displayed no discernible oxidation (GC data) after about a week. Samples are also stable when stored in a well-maintained glovebox.

Attempts to degas samples by simply evacuating vials containing a liquid sample for several hours and then sealing failed to remove the oxygen and significant oxidation occurred during subsequent storage after a few weeks. Samples stored under nitrogen in screw-capped vials in the laboratory—whether degassed or not—are vulnerable to autoxidation. In fact, *no reclosable container that protects such samples from autoxidation has been found to date*.

Oxygen is very soluble in organic compounds; the equilibrium concentration of oxygen in octane in equilibrium with air, for example, is 2.7 mM.[18] Oxygen has a particularly high solubility in fluorocarbon liquids,[19] and will diffuse through Teflon (which is a mass of compacted crystals) so that this material also is not an effective barrier to oxygen transport. Oxygen dissolves rapidly in organic liquids during transfers in air, but fortunately nonchain autoxidation processes are initially quite slow. The induction period that characterizes autoxidation reactions thus provides a "grace period" before rapid autoxidation commences, and this permits analyses and physical studies to be successfully performed.

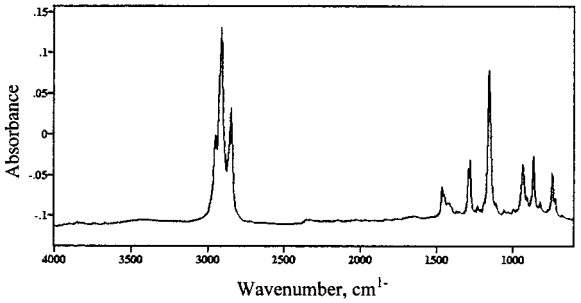

Figure 3. Powder ATR FT-IR spectrum of the equilibrium crystal of octyldimethylphosphine oxide, after adjusting intensities for angle of incidence and refractive indices (see Experimental Part).

NIR Microscope and Spectrometer. Infrared spectra were recorded by using an IR−PLAN microscope (Specra Tech, Inc.) integrated with a Mattson Galaxy 4050 FT-NIR spectrophotometer. The spectrophotometer was modified for use in the near-infrared by the use of a tungsten−halogen source, a calcium fluoride beam splitter, and a liquid nitrogen-cooled small-area In/Sb detector. The IR−PLAN microscope is fitted with redundant apertures above and below the sample, which were set to 50 μm × 250 μm and centered (with the long dimension oriented across the cell) to define the region of interest within the cell. Single-beam spectra were collected from first the reference cell (carbon tetrachloride) and then the sample, as double-sided interferograms at 4 cm^{-1} resolution. A mirror velocity of 40 cm/s was used. These two spectra were ratioed to obtain absorbance spectra spanning the frequency range of 7900 cm^{-1} to 1800 cm^{-1}. To achieve the desired signal-to-noise level, one hundred and twenty eight scans were coadded.

Positioning Stage. The DIT cell was positioned in the IR beam with a Motorized Micropositioning Stage (SpectraTech, Inc.). Computer-controlled stepper motors translate the stage platform in the $x-y$ plane with a resolution of 0.1 μm. The microscope platform was adjusted in the z direction to focus the sample. Preliminary focusing was performed with the optical objective in place; fine adjustments were made (by using illumination with visible light) through the IR objective lens.

Melting Point of Dry C_8PO. A cell containing dry C_8PO was prepared and the melting point determined by following the published revised phase science procedure for melting point determination.[20] It was found that this compound melts reversibly at 66.65 ± 0.05 °C. No liquid phase is visible just below its melting point (e.g., at 66.55 °C), and no birefringent crystals are visible just above its melting point (e.g., at 66.75 °C).

Infrared Studies of Dry C_8PO over a Temperature Range Spanning its Melting Point. A C_8PO DIT cell that had been loaded at least 1 day earlier was prepared, and a series of spectra were taken at successively higher 5 °C intervals until a temperature of 80 °C was reached. The direction of temperature change was then reversed and data again collected at the same intervals in the cooling direction.

A powder ATR spectrum of a sample of C_8PO that had stood for many months (and was presumed to be in its equilibrium state) was also taken by using a Ge ATR cell. The corrected spectrum of this material is shown in Figure 3. This was obtained from the raw spectrum by using the program "atrcorr.ab"

in Grams software. This program corrects for anomalies in spectral intensities by using the angle of incidence and approximate values for the refractive indices of the sample (taken to be 1.5) and of Ge (taken to be 4.0).

The frequencies of those C_8PO CH stretch bands that can be measured (i.e., were not too intense) were determined by using the 3-point algorithm of Cameron et al.[21] These frequency data are not absolute numbers because they depend on the algorithm used, but data determined by using the same algorithm should reflect systematic changes that occur as conditions are varied.

Discussion

Features of the DIT-NIR Method. The silica cells, cell loading procedures, and initiation procedures used in the earlier DIT-NDX method[1] are retained in the DIT-NIR method. Jamin−Lebedeff optics were retained for the qualitative examination of cells and also for cell calibration. These optics provide the most sensitive means known for visualizing index gradients within phases and also for seeing interfaces between phases. When a miscibility gap between coexisting phases is large, the discontinuity in indices is also typically large and seeing such interfaces is not a problem. When the miscibility gap is small, however, interfaces can be very difficult to see (especially when using bright-field illumination). This is especially true if the phases involved are either both isotropic or both birefringent.

DIT data have revealed that very small miscibility gaps are relatively common. Gaps of <1% (based on index data) have been found at the sponge liquid/cubic (L3/C) interface in the $C_{12}E_2$−water system,[12] at the cubic/lamellar (C/D) and cubic/cubic (C/C′) interfaces in the monoolein-water system,[22] and at the lamellar/liquid (D/L) interface in a polystyrene−polyoxyethylene−water system.[4] The width of the liquid/hexagonal (L/E) miscibility gap in the decyldimethylphosphine oxide−water system at 27 °C is 0.43% and at the hexagonal/liquid (E/L) boundary (both determined by using DIT-NIR data) is 0.58%. When one phase is birefringent and the other isotropic, recognizing the existence of a small miscibility gap is not a problem but determining its magnitude is.

It is worth noting that quantitatively determining small miscibility gaps by using classical methods is impossible because the boundary of the liquid crystal phase region is virtually impossible to accurately determine. Such measurements can be taken only by using swelling methods; thus, the amount of miscibility gap data is extremely small, and the significance of the widths of miscibility gaps cannot presently be addressed.

Determination of Water Composition by Using NIR Microspectroscopy. The distinctive feature of the new DIT-NIR method is the use of NIR microscopy to quantify water composition.[23,24] This is accomplished by using peak-area data on the OH bend−stretch combination band of water, obtained by integrating spectra between 4600 and 5400 cm^{-1}. This broad band, the peak of which lies near 5190 cm^{-1} (1.93 μm) but varies with conditions, is assigned to a combination band of the antisymmetric OH_2-stretching fundamental vibration (near 3600 cm^{-1}) and the OH_2-scissors deformation (near 1640 cm^{-1}).[25] Cells with a chamber thickness of 25 μm are far too thick for studies of fundamentals, but because first overtone and combination bands are generally 10 to 100 times less intense than are fundamentals, these cells have nearly ideal path lengths for quantitative measurements of these bands. (The peak absorbance of the combination band of pure water in a DIT cell is about 0.1 absorbance units). Because water is such an intense IR absorber, its combination band is much stronger than that of virtually all the other bands found in this region of the IR spectrum. Surfactants, for example, typically do not absorb strongly here. Even alcohols, polyols, and carboxylic acids, which have intense OH-stretching fundamental absorption (near 3600 cm^{-1}), show no IR absorption near 5200 cm^{-1}. This is because they lack the OH_2-deformation vibration near 1640 cm^{-1} found in water.

Both the cell material and the chamber thickness preclude spectral studies in the midrange IR. The cells are fabricated from fused silica, which is opaque at frequencies less than 2200 cm^{-1} and also between 3000 and 3700 cm^{-1}. Opacity in this region is due to OH absorption by residual silanol groups in the silica. Even in the spectroscopic window between 2200 and 3000 cm^{-1}, the 25 μm nominal chamber thickness is too large to permit quantitative studies.

Thermostated Oven. Accurate control of temperature is a must for phase studies, and excellent control had been achieved in the DIT-NDX method. However, the thermostated oven had to be redesigned to perform DIT-NIR studied. Whereas the DIT-NDX oven had a single slot with vertical walls for viewing the cell, the DIT-NIR oven has three slots—the outer two having beveled walls. One is used to view the sample cell, another to view the carbon tetrachloride reference cell, and the central slot is left open. The open slot (which retains the vertical walls) is used to determine the optics correction term during cell calibration and DIT-NDX phase studies.[1]

The walls of the first two slots are beveled at both the upper and lower surfaces to accommodate the conical illumination dictated by the low numerical apertures (0.71 condenser and 0.58 objective) and large diameters of the Cassegrainian lenses of the microscope. Unfortunately, beveling the walls compromises the temperature control somewhat. Temperature fluctuations are ±0.03 °C in the DIT-NIR oven, whereas they were only ±0.008 °C in the DIT-NDX oven.

Calibration. Octyldimethylphosphine oxide (C_8PO) was used to calibrate the peak-area of the water combination band vs composition. It is a superb calibration standard, for the following reasons:

An excellent laboratory synthesis of C_8PO exists.[15]

C_8PO is very stable thermally. It can be distilled in a vacuum, which permits the easy removal of nonvolatile impurities (such as electrolytes). It can be analyzed without derivatization by gas chromatography and by thin-layer and other forms of chromatography. The sample used in this work showed no detectable impurities by GC, infrared, or NMR analyses, but the limits of detection of impurities have not been established.

C_8PO is chemically inert to autoxidation and to all but the strongest oxidizing and reducing agents. Because it is transparent in the visible spectrum and absorbs light only weakly in the ultraviolet, it is unreactive photochemically.

The aqueous phase behavior of C_8PO (Figure 1) is ideal for calibration purposes. While hexagonal and lamellar liquid crystal phases do exist, they lie below room temperature so that only isotropic solutions exist over most of the temperature/composition range of interest. The crystal melts reversibly at 66.65 °C; above its melting point C_8PO is miscible with water in all proportions. The liquidus boundary extends downward from the melting point to below room temperature; at 25 °C it lies at 88%. The small triangular region within this miscibility gap is obviously not useful for calibration studies but is only a small percentage of the total area of the diagram between 25 °C and 80 °C.

Peak-area data were collected for homogeneous C_8PO−water mixtures between 25 and 80 °C. Samples were prepared at 5% composition intervals and mixed by using a small Teflon-clad

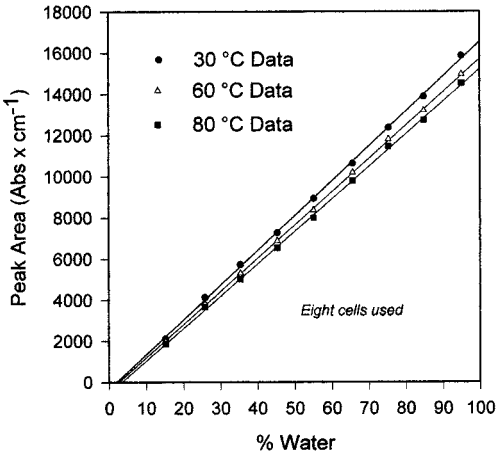

Figure 4. Peak area of the combination band of water vs octyldimethylphosphine oxide composition at three selected temperatures with linear regression lines. These data show the linearity with composition at each temperature and decreasing slope with increasing temperature.

magnetic stir bar to ensure homogeneity. Surprisingly long mixing times were required to fully equilibrate these samples. Although mixtures were homogeneous to the naked eye after a few minutes, DIT-NDX scans along the length of the cell demonstrated that perceptible gradients (of several percent per millimeter) existed for more than an hour. These disappeared after stirring for 2 h.

The DIT cells were filled by immersing one end of the open cell in the liquid, which slowly wicked into the chamber by capillary action. After sealing the ends, spectra were acquired at a known position (and chamber thickness) at 5 °C intervals between 25 °C and 80 °C. The peak-area data were normalized to 1 cm chamber thickness by using cell calibration data (determined by using interferometry). Data sets at three selected temperatures are shown in Figure 4. Several cells were used and scanning positions were selected randomly but always within the isothermal region (the middle 50% of the cell length).

The peak-area data were found to be proportional to composition at each temperature. The slopes of the calibration lines were found to display a power-law dependence on temperature. Given the linearity of the calibration data, it follows that the dependence on temperature of the peak-area of water itself dictates the dependence on temperature of the slopes of these lines. The peak-area data on water are accurately described by the algorithm

$$A_{\text{water}} = 17\,036 - 1.6273T^{-1.56}$$

$$r^2 = 0.9984$$

where A_{water} is the measured peak area per centimeter and T is the temperature (in °C). Combining this dependence of the peak area of water on temperature with the linear relationship between composition and peak area yields the following equation (shown graphically in Figure 5) for the dependence of solute composition on peak-area and temperature:

$$C = 100 - \left[\frac{100}{(a + bT^{1.56} - A_0) \times (A - A_0)}\right]$$

$$a = 17\,036;\ b = -1.6237;\ A_0 = -57$$

In this equation C is the solute (C_8PO) concentration (in weight percent), A is the peak area of a mixture (normalized to 1 cm chamber thickness), T is the temperature (in °C), and a, b, and A_0 are fitted parameters. A_0 reflects the nonlinearity in the baseline of the spectrum of dry phosphine oxide, as determined by integration between 4600 and 5400 cm^{-1}.

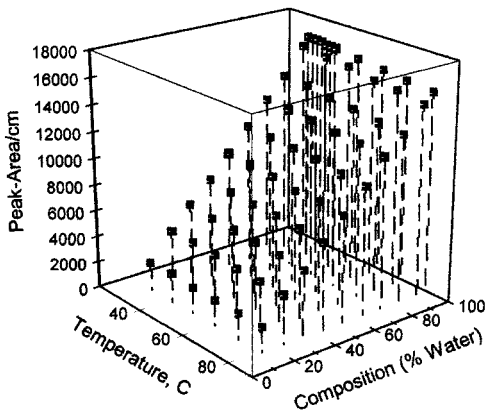

Figure 5. Composition-temperature-peak-area data for the octyldimethylphosphine oxide−water system over the temperature range 25 °C to 80 °C. Composition in mass fraction units.

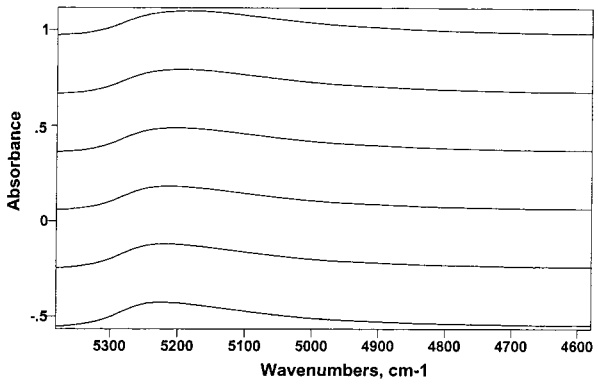

Figure 6. Combination band of water vs temperature from 30 °C (bottom spectrum) to 80 °C (top spectrum) in 10 °C increments.

These data could be said to obey Beer's law, except that this law as originally defined describes the linear relationship that exists between *absorbance* data a, concentration C, path-length l, and a specific absorbance extinction coefficient ϵ at a specific wavelength:[26,27]

$$a = \epsilon Cl$$

The above-described relationship differs in that a linear relationship is found to exist between *peak-area* data, concentration, path-length, and a specific peak-area extinction coefficient determined over a defined range of wavelengths.

Peak absorbance data from the calibration spectra are not nearly so well-behaved as are peak-area data. Figure 6 displays the combination band of water between 25 °C and 80 °C. Inspection of these data reveals that increasing the temperature of water sharpens the peak, shifts it to higher frequency (wavenumber), and *increases* the peak absorbance (Figure 7). These quantitative data reflect the qualitative difference in the dependence of peak-area on temperature (which decreases with increasing temperature) and absorbance (which increases with increasing temperature).

The form of the combination band varies with composition at a given temperature. Figure 8 shows stacked combination band spectra at 30 °C between 0% and 85% C_8PO. Changes in peak shape and frequency occur as composition is varied, and a shoulder at 5100 cm^{-1} appears at very low water/C_8PO ratios. The frequency at the peak of the combination band is poorly

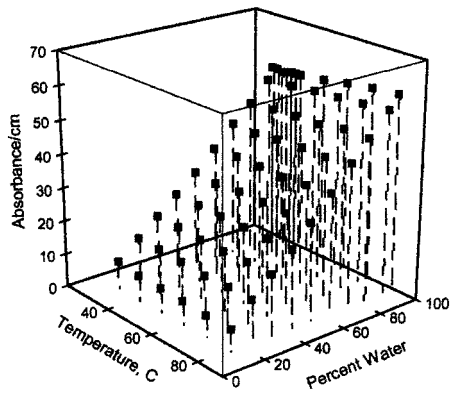

Figure 7. Peak absorbance of the combination band of water vs composition and temperature in octyldimethylphosphine oxide−water mixtures. Note that the absorbance at a given composition *increases* with increasing temperature, while the peak area (Figure 5) decreases.

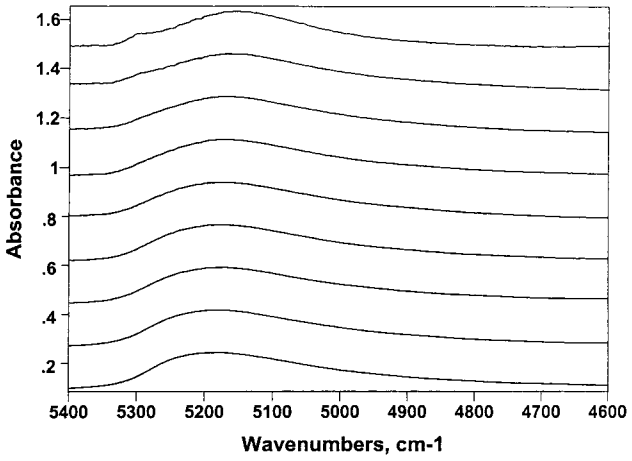

Figure 8. Combination band of water vs octyldimethylphosphine oxide composition along the 30 °C isotherm, from 5% (top spectrum) to 85% (bottom spectrum), in 10% increments.

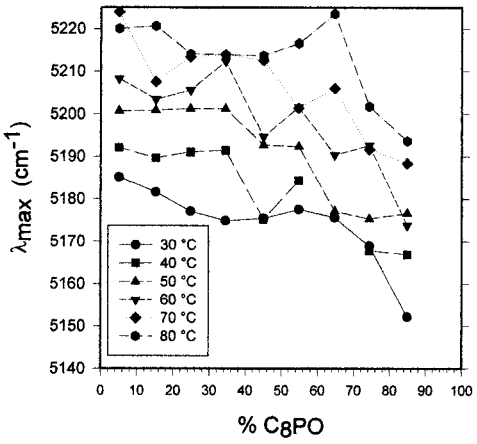

Figure 9. Frequency of the combination band of water vs composition at selected temperatures.

defined because the band is so broad. Its dependence on composition at various temperatures is complex (Figure 9).

Thermodynamic and infrared studies of hydrogen bonding in nonaqueous solvents have shown that phosphine oxides accept at least two hydrogen bonds of measurable strength from water. The first has an enthalpy of 7.8 kcal (33 kJ), which is significantly larger than the average hydrogen bond strength in liquid water (4.5 kcal, 19 kJ).[28] This is a characteristic feature

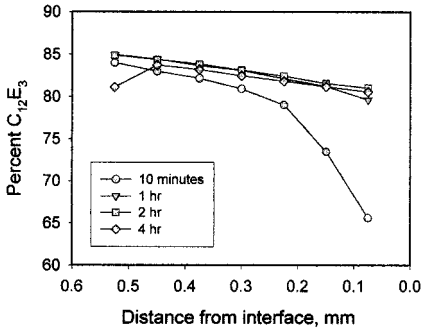

Figure 10. Time evolution of composition profiles during a DIT study of the trioxyethylene glycol monododecyl ether ($C_{12}E_3$)−water system.

of all operative hydrophilic groups, which always display stronger hydrogen bonding to water than water does to itself.[29] Hydrogen bond formation induces a shift in OH-stretching bands to lower frequencies; the frequency shift is a linear function of the enthalpy of the hydrogen bond.[30]

The observed changes in the water spectra along isotherms are fully consistent with earlier data because the peak frequency of the OH-combination band envelope is shifted to lower frequencies as the concentration of C_8PO increases. This is to be expected because the fraction of water that is hydrogen bonded to the phosphoryl group must steadily increase as the molecular ratio of water to C_8PO decreases. These data are also consistent with information suggesting that increasing the temperature decreases the level of structure that exists in liquid water,[31] and also increases the proportion of non-hydrogen-bonded OH groups that exist.

The thermodynamic state of water evidently varies with temperature, and this affects the peak-area extinction coefficient of the water combination band. At a defined temperature, however, the peak-area extinction coefficient of water is evidently unaffected by composition. Other data (see validation section) indicate that the specific peak-area coefficient is also independent of the chemical structure of the solutes present ($C_{12}E_3$ vs C_8PO). Taken as a whole, these data suggest that (at a given temperature) *substantial variations in the thermodynamic state of water may occur without influencing the peak-area extinction coefficient of the water combination band*. This result is significant with respect to the physical science of functional group hydration. Analytically, a simpler and more useful result can hardly be imagined.

Influence of Time on Band Profiles. The composition limits of a phase correspond to the compositions at the interfaces at either end of its phase band. Swelling experiments are dynamic, and both the positions of interfaces and the shapes of composition profiles change constantly with time. When two phases coexist, however (as at an interface), and when temperature and pressure are fixed, compositions are invariant within a binary system. Compositions at interfaces cannot be determined directly because of the complex refraction that occurs there, but data at known distances from an interface can be determined and extrapolated to the position of the interface. Figure 10 shows the time evolution of composition profiles at the L2(L2/D) boundary in the $C_{12}E_3$−water system. Note that the nomenclature system for miscibility gaps suggested earlier[10] is used here. A particular miscibility gap is defined by stating first the dilute phase and then the concentrated phase, separated by a slash. To designate one particular phase, the designation of the gap is placed in parentheses and the phase of interest is indicated before the parentheses. Thus the concentrated phase at the D/L2 miscibility gap is uniquely designated as L2(D/L2). Although

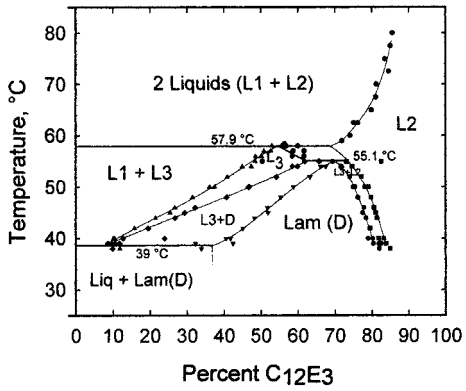

Figure 11. Phase diagram of the trioxyethylene glycol monododecyl ether ($C_{12}E_3$)−water system. Reproduced with permission (ref 10).

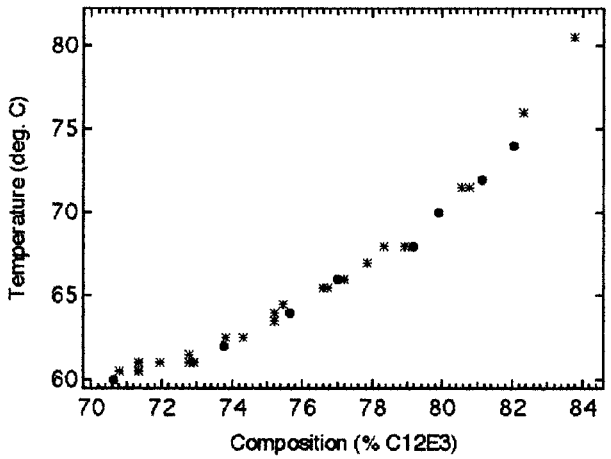

Figure 12. A comparison of isothermal DIT-NIR and isoplethal SWD data on the location of the L2 boundary in the $C_{12}E_3$−water system.

the composition profile within the phase band changes with time, the compositions at the interfaces remain constant (as was also found earlier in the $C_{10}E_4$−water system[1]). Better quantitative estimates of the compositions at interfaces are obtained by allowing concentration gradients to flatten (after initiating the cell) before composition profiles are determined.

DIT-NIR Method Validation. To validate the generality of the DIT-NIR method, selected phase boundaries in the trioxyethylene glycol monododecyl ether ($C_{12}E_3$)−water system were determined by using three different phase-study methods: DIT-NDX, DIT-NIR, and the stepwise dilution (SWD) isoplethal method. The phase diagram of this system has been reported[10] and is reproduced in Figure 11. $C_{12}E_3$ is attractive for validation because two phase boundaries exist (the L2(L1/L2) and L2(D/L2) boundaries) that can be investigated by using all three methods. Moreover, well-behaved swelling is observed at these two interfaces so that accurate extrapolations of DIT data to interface positions is possible. The L2 phase is isotropic, which facilitates use of the SWD method. Heating this phase to above the L2(L1/L2) boundary results in abrupt clouding, while cooling to below the L2(D/L2) boundary results in precipitation of the birefringent lamellar (D) phase. These boundaries were therefore carefully determined by using the DIT-NIR and SWD methods, and a partial phase study was conducted by using the DIT-NDX method.

The DIT-NIR and SWD data are shown in Figure 12; good agreement is found between data obtained by the two methods. The agreement was particularly good for the L2(L1+L2) phase because the clouding associated with this phase transition is abrupt and the boundary temperature could easily be determined.

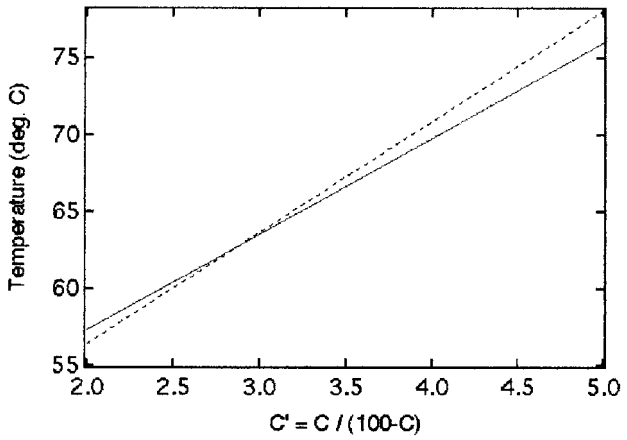

Figure 13. A statistical comparison of the DIT-NIR and SWD data on the L2(L1+L2) boundary.

TABLE 1: Comparison of L2 Boundary Concentrations at Selected Temperatures by Different Methods

temp, °C	% $C_{12}E_3$ by SWD method	% $C_{12}E_3$ by NIR method	% $C_{12}E_3$ by NDX method	C(NDX)-C(NIR)
62.0	73.36	73.76	64.53	−9.23
60.0	72.16	70.62	58.35	−12.27
54.0	77.09	73.93	57.79	−16.14

The scatter observed in the SWD data associated with the L2-(D+L2) phase results from the greater difficulty encountered in determining the exact temperature at which the D phase is formed. When observed between crossed polarizers, the sample first lightens uniformly before a "definitive" domain of D phase is seen. Despite these difficulties, the differences in composition/temperature coordinates between the DIT-NIR and the SWD data are small on an absolute basis.

The L2/(L1/L2) data from the two methods were also compared by fitting them to a linear model and comparing the predicted lines (Figure 13). To do this, the data were first transformed to the function $c' = c/(100-c)$, where c is composition. This transformation creates a nearly linear data set that is well-described by using linear regression. The computed slopes for each data set are significantly different but within the region of principal interest ($c' < 4$ or $c < 80\%$) the differences are not statistically significant. The slopes are significantly different for $c' > 4$, but these data fall at high temperatures where the variability of both methods is relatively large.

The $C_{12}E_3$-water system was also studied by using the DIT-NDX method. The estimated compositions of the L2 phase at three selected temperatures are shown in the Table 1. Significant and variable differences can be seen between the DIT-NDX data, on one hand, and the DIT-NIR/SWD data on the other. The data in this table, together with the erratic behavior of the indices of birefringent phases, document the basis for developing the DIT-NIR method.

Other Information from Spectral Data; Infrared Studies of Dry C_8PO over a Temperature Range Spanning Its Melting Point. The use of spectral (in place of interferometric) data for phase studies introduces an entirely new dimension to these studies because infrared band frequency data can provide information regarding the physical state of the sample. An example of such auxiliary physical studies can be seen from spectral data taken in both the heating and the cooling directions on dry C_8PO, over a temperature range spanning its melting point. In Figure 14, band frequency data on a C_8PO cell that had been loaded about a day earlier are presented. A series of spectra was first taken at successively higher 5 °C intervals

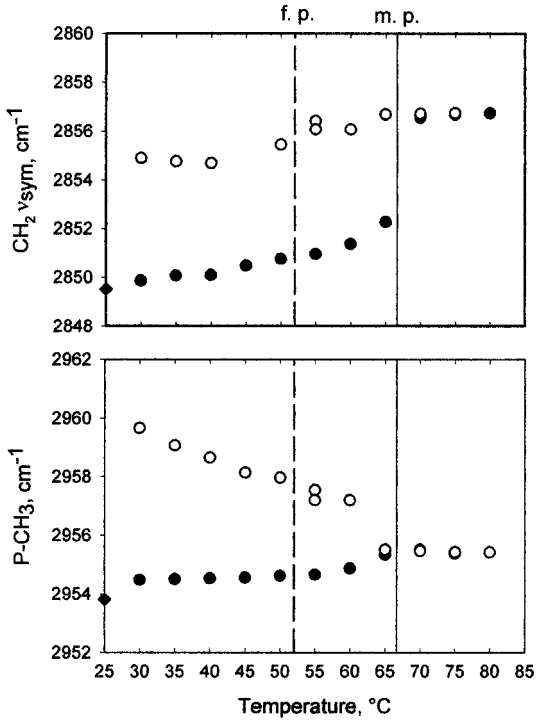

Figure 14. Band frequency data for the symmetric CH_2 and the P−CH_3 bands of dry octyldimethylphosphine oxide vs temperature, between 25 °C and 80 °C. Open symbols represent data taken in the heating direction, and closed symbols represent data taken in the cooling direction. Melting point temperature—vertical solid line. Freezing point temperature—vertical dashed line.

between 25 °C and 80 °C. The direction of temperature change was then reversed and data were again collected at the same intervals. The powder Attenuated Total Reflectance (ATR) spectrum of C_8PO (after adjustment of band intensities for anomalies introduced by ATR) is shown in Figure 3. This sample had stood at room temperature for many months and was expected to be in its equilibrium state.

Shown in Figure 14 (see Supporting Information) are peak frequency data for the symmetric CH_2 stretch and the P−CH_3 bands vs temperature. Vertical solid or dashed lines indicate melting and freezing temperatures. Data taken in the heating direction are shown by open circles and data taken in the cooling direction by filled circles. The filled diamond data point was taken from the above-mentioned ATR spectrum of the equilibrium sample. The similarity of the ATR data to the frequencies of the sample in the DIT cell (which had been melted and refrozen the previous day) suggests that equilibration of this crystal after melting and refreezing occurs within approximately a day's time.

A smooth increase in frequency of the symmetric CH_2 band occurs with increasing temperature, and an upswing is observed just below the melting point. On passing the melting point, band frequencies jump to higher values characteristic of the liquid phase. Band frequencies in the liquid are barely influenced by a further increase in temperature. Because they are identical in both the heating and cooling directions, they appear to be equilibrium values. The upswing below the melting point suggests the existence of a "*pretransition endotherm*." This result is consistent with much evidence that fatty crystals in equilibrium with their melt are structurally disordered, relative to the perfect single crystal.[32] If so, they also necessarily possess an elevated enthalpy (and free energy) relative to the single crystal. This disorder diminishes at temperatures far below the melting point. This phenomenon has been discussed elsewhere but in different terms (as a "premelting" or partial melting transition).[33]

Supercooling was observed below the melting point down to the temperature indicated by the vertical dashed line. Frequency data below the melting point are remarkably similar to those of the equilibrium liquid—*even after freezing occurs.* Liquid-like frequencies are observed down to room temperature, which suggests that the chain conformational structure of the frozen melt initially closely resembles that of the equilibrium liquid. The molecules appear to rapidly freeze into a solid but highly disordered state, and then relax more slowly to the conformation of the equilibrium crystal phase (which is presumably all trans) within about a day's time.

The behavior of the P−CH_3 band associated with the headgroup is particularly interesting. As with the chain CH_2 bands, the frequency of the P−CH_3 band slowly rises on heating, shows an upswing just below the melting point and a small discontinuity at the melting point, and is constant and reversible in the liquid phase. However, this band unexpectedly displays a strong *increase* in frequency as the temperature of the frozen solid decreases to room temperature; it is substantially *higher* at 25 °C than it is in the liquid phase. This band thus resembles that which may exist in the gas phase. These data suggest the hypothesis that freezing the melt initially locks the chains together but pulls the headgroups apart. Further studies of this unproven phenomenon are evidently warranted.

Conclusions

The advent of quantitative isothermal swelling phase study methods[1] has added a new dimension to the phase science of surfactants. The powerful X-ray tools used in conjunction with swelling studies by Caffrey[34−36] and by Kekicheff[37] provided information of unprecedented quality on the structures of the phases that exist, but recourse to cumbersome quantitative methods (e.g., calorimetry) was required to determine boundary compositions. The availability of a reliable quantitative isothermal swelling method would both complement these phase-structure-oriented methods and enhance the reliability of phase studies.

DIT-NIR retains all the advantages of the earlier DIT-NDX method, yields boundary composition data of acceptable quantitative accuracy (ca. ±0.5%) in binary aqueous systems, and in addition provides useful spectral data. The linear dependence on composition of the peak-area data of the OH-bend−stretch combination band, plus the fact that this band is unique to the water molecule, make DIT-NIR extremely attractive. Unpublished studies of other surfactants (and even of concentrated protein solutions) suggest that the determination of water by this method may be independent of the nature of the solutes present.

Anomalous swelling compromises DIT of poorly soluble surfactants at the L1+D interface when the D phase is dilute.[6,7] Anomalous swelling is of considerable contemporary interest because it is closely related to the phenomenon of "spontaneous vesicle formation".[6] As noted in the Introduction, swelling studies intended at the outset to yield equilibrium phase data have, on numerous occasions, revealed important information on nonequilibrium (kinetic or colloidal) phenomena.[7−9] Swelling methods are applicable in principle to ternary systems.[4] Indeed, the first quantitative ternary phase study based on the swelling principle has recently been reported,[38] but more work is necessary here.

Beyond determining the compositions of coexisting phases, DIT-NIR can provide information on the vibrational states of

the molecules present. The anomalies in the water band that result from perturbations caused by the hydrophilic groups present is one aspect of this information. Another is illustrated by the data (above) on dry C_8PO during the melting and freezing processes, which is based on changes in the frequencies of CH-stretching fundamentals. These bands are perturbed to a measurable degree by the phase state within which molecules exist and reflect changes of state from crystal to fluid (liquid or liquid crystal). Infrared frequency data can provide insight into both equilibrium liquids and crystals and also nonequilibrium solid states. Data on frequency shifts may possibly provide a means of scaling deviations from equilibrium because it has been suggested that these frequencies are dictated by the trans:gauche conformer ratio in chains.[39] Considerable interest presently exists in the study of polymers and other long-chain compounds by using vibrational spectroscopy.[40,41]

Studies using HOD could further extend the value of DIT-NIR studies. It has been firmly established that the mixed isotope of water displays more symmetrical and easily interpreted stretching bands than do either HOH or DOD.[42] Both the O−H and the O−D stretching bands of HOD can be seen in the DIT cell. DIT-Raman studies are also feasible because DIT cells are transparent to the light used for Raman excitation. One such study has already been reported.[43]

Acknowledgment. The $C_{12}E_3$ sample was prepared by G. M. Bunke using the modified Williamson synthesis of Gibson.[44] Bunke also collaborated in development of the low-temperature closed pressure filters used for recrystallization and methods for using them. B. J. King performed the preliminary phase studies of $C_{12}E_3$. K. D. Juhlin performed the statistical comparisons of experimental data on the $C_{12}E_3$ boundary. G. M. Story performed the ATR FT-IR infrared studies of the dry C_8-PO, and the adjustments of this spectrum.

Supporting Information Available: Detailed information on the construction and use of the DIT-NIR apparatus. This information is available free of charge via the Internet at http://pubs.acs.org.

References and Notes

(1) Laughlin, R. G.; Munyon, R. L. *J. Phys. Chem.* **1987**, *91*, 3299−3305.
(2) Gerritsen, H. C.; Caffrey, M. *J. Phys. Chem.* **1990**, *94*, 944−948.
(3) Laughlin, R. G. *J. Am. Oil Chem. Soc.* **1990**, *67*, 705−710.
(4) Laughlin, R. G. *Adv. Colloid Interface Sci.* **1992**, *41*, 57−79.
(5) Laughlin, R. G.; Fu, Y.-C.; Wireko, F. C.; Scheibel, J. J.; Munyon, R. L. In *Novel Surfactants*, Holmberg, K., Ed.; Marcel Dekker: New York, 1998; pp 1−30.
(6) Laughlin, R. G. *Colloids Surf. A: Physicochem. Eng. Aspects* **1997**, *128*, 27−38.
(7) Laughlin, R. G.; Munyon, R. L.; Burns, J. L.; Confindaffer, T. W.; Talmon, Y. *J. Phys. Chem.* **1992**, *96*, 374−383.
(8) Laughlin, R. G.; Munyon, R. L.; Fu, Y.-C.; Fehl, A. J. *J. Phys. Chem.* **1990**, *94*, 2546−2552.
(9) Laughlin, R. G.; Munyon, R. L.; Fu, Y. C.; Emge, T. J. *J. Phys. Chem.* **1991**, *95*, 3852−3856.
(10) Laughlin, R. G. In *Micelles, Microemulsions, and Monolayers: Science and Technology*; Shah, D. O., Ed.; Marcel Dekker: New York, 1998; pp 73−100.
(11) Gray, G. W. *Molecular Structure and the Properties of Liquid Crystals*, Academic Press: New York, 1962. *Macroscopic and Technical Properties of Matter: Group IV. Liquid Crystals: Transition Temperatures and Related Properties of Three-ring Systems with One Bridging Group*; Thiem, J., Vill, V., Eds.; Landolt-Boernstein: Numerical Data and Functional Relationships in Science and Technology Series; Springer-Verlag: Berlin, Subvol D, 1994, Subvol E, 1995.
(12) Lynch, M. L. *Langmuir* **2000**, *16*, 3537−3542.
(13) Laughlin, R. G.; Marrer, A. M.; Marcott, C.; Munyon, R. L. *J. Microsc.* **1985**, *139*, 239−247.
(14) F. J. Bates and Associates. *Polarimetry, Saccharimetry, and the Sugars*; U. S. Government Printing Office: Washington, DC, 1942; pp 254−261.
(15) Hays, H. R. *J. Org. Chem*. **1968**, *33*, 3690−3694.
(16) Laughlin, R. G. *J. Colloid Interface Sci.* **1976**, *55*, 239−241.
(17) Knapp, D. R. *Handbook of Analytical Derivatization Methods*; Wiley & Sons: New York, 1979.
(18) Thomsen, E. S.; Gjaldbaek, J. Chr. *Acta Chem. Scand*. **1963**, *17*, 127−133. Markham, A. E.; Kobe, K. A. *Chem. Rev.* **1941**, *28*, 519−585. Battino, R.; Clever, A. H. L. *Chem Rev.* **1966**, *66*, 519−588.
(19) Zander, R. *Res. Exp. Med.* **1974**, *164*, 97−109.
(20) Laughlin, R. G. *The Aqueous Phase Behavior of Surfactants*; Academic Press: London, 1994; pp 523−525.
(21) Cameron, D. G.; Kauppinen, J. K.; Moffatt, D. J.; Mantsch, H. H. *Appl. Spectrosc.* **1982**, *36*, 245−250.
(22) Laughlin, R. G. In *Food Emulsions and Foams: Theory and Practice*; Gaden, D. L., Series Ed., Wan, P. J., Volume Ed.; American Institute of Chemical Engineers: New York; Vol. 86, pp 7−15.
(23) Marcott, C.; Laughlin, R. G.; Sommer, A. J.; Katon, J. E. In *ACS Syposium Series, FTIR Spectroscopy in Colloid and Interface Science*; Scheuing, D. R., Ed.; American Chemical Society: Washington, DC, 1991; pp 71−86.
(24) Marcott, C.; Munyon, R. L.; Laughlin, R. G. *SPIE 8th International Conference on Fourier Transform Spectroscopy*, Vol. 157; Society of Photooptic Instrumentation Engineers: Bellingham, WA, 1992; pp 290−291.
(25) Herzburg, G. *Infrared and Raman Spectra*; Van Nostrand Reinhold: New York, 1945; p 281.
(26) Colthup, N. B.; Daly, L.; Wiberly, S. E. *Introduction to Infrared and Raman Spectroscopy*, 3rd ed.; Academic Press: London, 1990; pp 100−103.
(27) Willard, H. H.; Merritt, L. L., Jr.; Dean, J. A.; Settle, F. A., Jr. *Instrumental Methods of Analysis*, 6th ed.; D. Van Nostrand Co.: New York, 1981; pp 66−71.
(28) Laughlin, R. G. In *Advances in Liquid Crystals*, Vol. 3; Brown, G. H., Ed.; Academic Press: New York, 1978; pp 93−97.
(29) Laughlin, R. G. *The Aqueous Behavior of Surfactants*; Academic Press: London, 1994; pp 259−327.
(30) Joesten, M. D.; Schaad, L. J. *Hydrogen Bonding*; Marcel Dekker: New York, 1974.
(31) Walrafen, G. E. In *Water, a Comprehensive Treatise*, Vol. I; Franks, F., Ed.; 1972; pp 151−214.
(32) Small, D. M. *The Physical Chemistry of Lipids. From alkanes to phospholipids*. *Handbook of Lipid Research*; Plenum Press: New York, 1986; pp 191−219.
(33) Skau, E. L. *J. Chim. Phys.* **1934**, *31*, 366−382. Sturtevant, J. M. In *Physical Methods of Organic Chemistry*, 3rd ed. Weissberger, A., Ed.; Interscience Publishers: New York, 1939; Vol. I, Part I, pp 556−557.
(34) Caffrey, M. *Biophys. J.* **1987**, *51*, 444a.
(35) Caffrey, M. *Biophys. J.* **1989**, *55*, 47−52.
(36) Caffrey, M.; Bywater, M. T. *J. Soc. Cosmet. Chem*. **1988**, *39*, 159−67.
(37) Kekicheff, P.; Grabielle-Madelmont, C.; Ollivon, M. *J. Colloid Interface Sci*. **1989**, *131*, 112−132.
(38) Ricoul, F.; Dubois, M.; Zemb, T.; Vandais, A.; Noel, J. P.; Lefevre, M.; Plusquellec, D.; Diat, O. *Prog. Colloid Polym. Sci*. **1997**, *105*, 351−359.
(39) Snyder, R. G. *J. Chem. Soc., Faraday Trans*. **1992**, *88*, 1823−1833.
(40) Zerbi, G.; Del Zoppo, M. *J. Chem. Soc., Faraday Trans.* **1992**, *88*, 1835−1844.
(41) Snyder, R. G.; Maroncelli, M.; Strauss, H. L.; Elliger, C. A.; Canera, D. G.; Casal, H. L.; Mantsch, H. H. *J. Am. Chem. Soc*. **1983**, *105*, 133−134.
(42) Wong, P. T. T.; Moffatt, D. *J. Appl. Spectrosc*. **1987**, *41*, 1070−1072.
(43) Andrew, J. J.; Clark, I. E.; Millichore, A. J. *Proceedings of the 15th International Conference on Raman Spectroscopy*; Wiley & Sons: New York, 1996; p 1166.
(44) Gibson, T. *J. Org. Chem.* **1980**, *45*, 1095−1098.